8-2021

Effects of tidal flooding on estuarine biogeochemistry: Quantifying flood-driven nitrogen inputs in an urban, lower Chesapeake Bay sub-tributary

Alfonso Macías-Tapia

Margaret R. Mulholland

Corday R. Selden

Jon Derek Loftis

Peter W. Bernhardt

Water Research 201 (2021) 117329

Contents lists available at ScienceDirect

Water Research

journal homepage: www.elsevier.com/locate/watres

Effects of tidal flooding on estuarine biogeochemistry: Quantifying flood-driven nitrogen inputs in an urban, lower Chesapeake Bay sub-tributary

Alfonso Macías-Tapia [a,*], Margaret R. Mulholland [a], Corday R. Selden [a,1], J. Derek Loftis [b], Peter W. Bernhardt [a]

[a] Department of Ocean and Earth Sciences, Old Dominion University, Norfolk, VA, USA
[b] Center for Coastal Resources Management, Virginia Institute of Marine Science, College of William and Mary, Gloucester Point, VA, USA

ARTICLE INFO

Keywords:
Sea level rise
Tidal flooding
Nitrogen loading
Water quality
Enterococcus
King tide

ABSTRACT

Sea level rise has increased the frequency of tidal flooding even without accompanying precipitation in many coastal areas worldwide. As the tide rises, inundates the landscape, and then recedes, it can transport organic and inorganic matter between terrestrial systems and adjacent aquatic environments. However, the chemical and biological effects of tidal flooding on urban estuarine systems remain poorly constrained. Here, we provide the first extensive quantification of floodwater nutrient concentrations during a tidal flooding event and estimate the nitrogen (N) loading to the Lafayette River, an urban tidal sub-tributary of the lower Chesapeake Bay (USA). To enable the scale of synoptic sampling necessary to accomplish this, we trained citizen-scientist volunteers to collect 190 flood water samples during a perigean spring tide to measure total dissolved N (TDN), dissolved inorganic N (DIN) and phosphate concentrations, and *Enterococcus* abundance from the retreating ebb tide while using a phone application to measure the extent of tidal inundation. Almost 95% of *Enterococcus* results had concentrations that exceeded the standard established for recreational waters (104 MPN 100 mL^{-1}). Floodwater dissolved nutrient concentrations were higher than concentrations measured in natural estuarine waters, suggesting floodwater as a source of dissolved nutrients to the estuary. However, only DIN concentrations were statistically higher in floodwater samples than in the estuary. Using a hydrodynamic model to calculate the volume of water inundating the landscape, and the differences between the median DIN concentrations in floodwaters and the estuary, we estimate that 1,145 kg of DIN entered the Lafayette River during this single, blue sky, tidal flooding event. This amount exceeds the annual N load allocation for overland flow established by federal regulations for this segment of the Chesapeake Bay by 30%. Because tidal flooding is projected to increase in the future as sea levels continue to rise, it is crucial we quantify nutrient loading from tidal flooding in order to set realistic water quality restoration targets for tidally influenced water bodies.

1. Introduction

Sea level rise (SLR) has severely impacted low-elevation coastal areas world-wide, causing more frequent and severe inundations during tidal flooding events (Nicholls and Cazenave, 2010). Coastal flooding in the Lower Chesapeake Bay region has accelerated because rates of relative sea level rise along the U.S. East Coast are about 30% higher than the global average (Ezer and Atkinson, 2014) due to the combination of long-term anthropogenic sea level rise (Tebaldi et al., 2012), local subsidence (Ezer and Corlett, 2012), natural climate variability (Ezer et al., 2013), and changes in oceanic circulation affecting the adjacent Gulf Stream (Ezer et al., 2013). As a result, the hours per year with water levels 0.5 m above mean higher high water (MHHW) have increased dramatically (Ezer et al., 2018). Relative SLR for the region also appears to be accelerating (Boon and Mitchell, 2015; Boon et al., 2018), suggesting that the severity of tidal flooding will continue to increase in the foreseeable future. For example, Spanger-Siegfried et al. (2014) reported that 30 of 52 cities along the northeast coast of the US

* Corresponding author.
E-mail address: amaciast@odu.edu (A. Macías-Tapia).
[1] Present address: Department of Marine and Coastal Sciences, Rutgers University, New Brunswick, NJ, USA.

https://doi.org/10.1016/j.watres.2021.117329
Received 22 February 2021; Received in revised form 29 May 2021; Accepted 1 June 2021
Available online 4 June 2021

are predicted to have more than 20 tidal flooding events each year that will cause considerable impact (e.g., closure of roads and damage to infrastructure) by the year 2030 and more than 50 events per year by 2045, including some extreme cases that are predicted to have more than 250 tidal flooding events per year by 2045.

Because of its gravitational forcing, tidal flooding can occur at high tide in the absence of rain (i.e., "blue sky" flooding) and can be predicted with high precision (Loftis et al., 2019). Meteorological forcing (e.g., wind speed and direction) and ocean circulation (e.g., strength of western boundary currents) can exacerbate or ameliorate tidal height independent of gravitational forcing (Ezer et al., 2013; Ezer, 2018) and this is predicted with less precision and on shorter timescales. Most studies examining impacts of tidal flooding have focused on threats to resources on land, such as urban infrastructure and human health (Li et al., 2013; Ching-Pong et al., 2018; Akpinar-Elci et al., 2018), and wetlands (Raposa et al., 2016). However, little is known about water quality impairments to adjacent aquatic ecosystems that result from recurrent tidal flooding in urban areas. While estimates of stormwater inputs into coastal systems have been made (e.g., Hale et al., 2015), exchanges of materials (e.g., sediment, nutrients, and fecal matter) between coastal lands and adjacent aquatic systems as a result of tidal flooding have not been quantified.

Efforts to restore the Chesapeake Bay have been ongoing since 1985. However, because voluntary restoration activities failed to achieve their goals by 2010, the restoration was placed under federal mandate. To achieve restoration targets, the U.S. Environmental Protection Agency (EPA) established segment-specific total maximum daily loads (TMDLs) for the entire Chesapeake Bay watershed (Wainger, 2012). These load allocations were designed to be protective of water quality impairments that impede recreational and commercial use of its resources, including low dissolved oxygen (hypoxic/suboxic zones), accumulation of fecal contaminants, low water clarity, and excessive algal biomass (Wainger et al., 2013). Limits were established for nitrogen (N) and phosphorus (P) loads because these two elements have been recognized as essential nutrients for phytoplankton growth (Downing 1997; Bristow et al., 2017) and excess algal growth has been linked to reduced water clarity, and the development of hypoxic/anoxic waters through the creation of biological oxygen demand (Hagy et al., 2004).

The TMDLs also allocate nutrient loads by sector, establishing load allocations for wastewater treatment facilities, industrial discharges, atmospheric deposition, and other point and non-point land-based sources (e.g., runoff). The land-based load allocation is primarily from stormwater inputs and associated runoff. Nutrients delivered to the watershed during coastal flooding in the absence of rainfall are not currently accounted for in these allocations. When areas are inundated as a result of coastal flooding, materials that have accumulated on the landscape can be carried into waterways when floodwaters recede (Pandey et al., 2014; Köhler et al., 2013; Selbig, 2016). Further, due to the amount of time tidal floodwaters remain on the landscape (i.e., hours), biogeochemical reactions may alter the composition of nutrient elements within the floodwaters or mobilize material on the landscapes or in soils, facilitating its delivery to the estuary. Quantifying nutrient inputs from coastal flooding and including these inputs in the TMDL is of paramount importance for accurately calculating nutrient loads, and their potential water quality impacts, to low-lying tidal regions of the Chesapeake Bay watershed. If nutrient loads delivered during tidal flooding events are substantial, this could jeopardize the realization of water quality restoration goals.

Here, we provide the results of a study in which the objective was to provide the first extensive spatial characterization of nutrient concentrations from tidal floodwaters and estimate nutrient loading during a "blue sky" tidal flooding event in the Lafayette River, a sub-tributary of the lower Chesapeake Bay. This was made possible by leveraging a citizen-science project that enabled tributary-wide, intensive, and synoptic sample collection during a tidal flooding event in 2017 associated with a perigean spring tide (i.e., king tide). We measured dissolved N and P concentrations in water samples collected from the receding high tide, corrected these for concentrations already present in the estuarine water prior to its encroachment onto the land, and combined these with modeled estimates of floodwater volume to calculate nutrient loading to the Lafayette River from a tidal flooding event to test the hypothesis that floodwaters from an urban landscape are a net source of dissolved nutrients to the estuary.

2. Methods

2.1. Study site

The Lafayette River watershed is a sub-tributary of the lower Chesapeake Bay located completely within the city of Norfolk, VA (Fig. 1). Most of its watershed is prone to flooding because elevations are less than 5 m above mean sea level (Fig. 1 and Kleinosky et al., 2007). Long-term water level data indicate that tidal flooding will become more frequent and intense in the future (Spanger-Siegfried et al., 2014; Ezer, 2018).

2.2. Floodwater sample collection and processing

During the perigean spring tide (i.e., king tide) that occurred on November 5, 2017 (Fig. 1), public and private media outlets and a non-profit group located in Norfolk, VA, organized a crowd-sourced citizen science sampling event ('Catch the King') that set a Guinness world record for 'Most contributions to an environmental survey' (Loftis et al., 2019). This project was made possible by the development of a smartphone application (Sea Level Rise, Concursive Corporation) funded by the non-profit group Wetlands Watch (http://wetlandswatch.org/). The application allows users to report the extent of tidal flooding, by walking along the water's edge and periodically (e.g., every five steps) pressing a button on their smart phone to drop "pins" that are data that include the geographic coordinates at the water's edge and the associated time and date of data collection. The phone application also allows the user to save pictures and comments associated with data points.

In parallel with the inaugural Catch the King event in 2017, we trained a subset of volunteers to collect water samples from the retreating floodwaters while also using the phone application to measure the extent of tidal inundation. Volunteers primarily included high school students taking advanced placement environmental science, their teachers and parents, and graduate and undergraduate students (graduate and undergraduate), faculty, and staff from Old Dominion University. These volunteers collected 190 floodwater samples within an hour of high tide.

Teams of volunteers were trained to use the phone application before the king tide event. On the day of the event, sampling teams were provided with acid-cleaned sample bottles, gloves, sample log sheets to record metadata, coolers with ice packs to store samples, and instructions for sample collection and data recording using the provided log sheets and the Sea Level Rise phone application. Each team was then assigned to sample in a specific part of the watershed where flooding was expected based on output from the Tidal Inundation Tracking Application for Norfolk (TITAN) model (http://gisapp1.norfolk.gov/TITAN/HOME.aspx). Samples were transported in the coolers to Old Dominion University, Norfolk, VA, where salinity was measured immediately using refractometers, and then water samples filtered through pre-combusted glass fiber filters (Whatman GF75; nominal pore size of 0.3 μm) and frozen for later analysis of nutrient concentrations (see below). Pictures, sample identifiers and location data, and salinity results were used to confirm that samples were collected from floodwater.

From 40 sampling sites, floodwater samples were collected in autoclave-sterilized glass 250 mL bottles for enumeration of *Enterococcus* abundance by the Hampton Roads Sanitation District or the Virginia Department of Health within 24 h of sample collection.

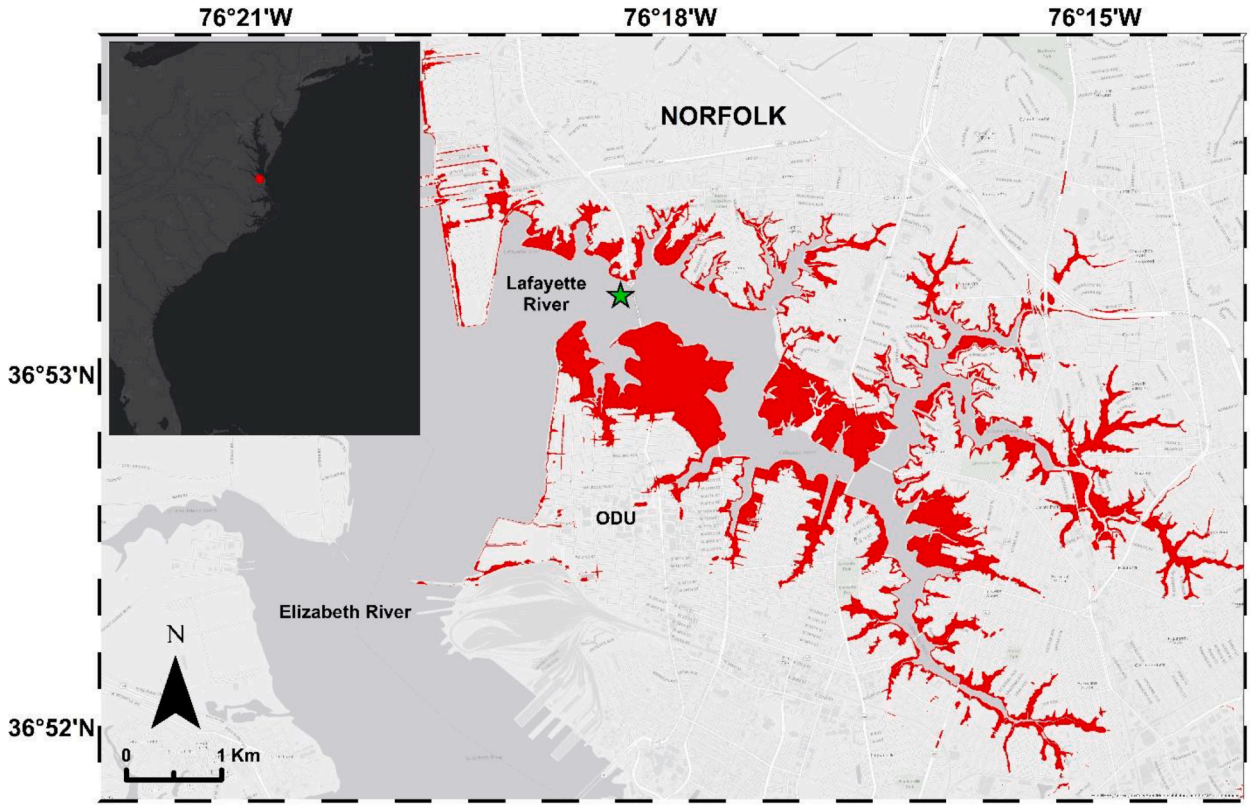

Fig. 1. Flooding produced at the perimeter of the Lafayette River when the water level is 1 m above mean lower low water (MLLW). Data source for flood projection: City of Norfolk – Open Data Portal (https://www.norfolk.gov/3885/Open-Data-Norfolk). The star represents the site where in-river samples were collected prior to floodwater sampling. Inset shows the Atlantic coast of the continental US and the location of the city of Norfolk, in the mid-Atlantic region (red area) (For interpretation of the references to color in this figure legend, the reader is referred to the web version of this article.).

2.3. Estuarine sample collection

Surface (<0.25 m) water samples were collected almost daily, between August 1 and September 10, 2017, at a site near the mouth of the Lafayette River (Fig. 1; a total of 39 samples). Samples were collected directly into 15 mL Falcon® tubes, using a peristaltic pump connected to a Whatman® 0.8/0.2 μm pore-size filter, transported in a cooler with ice to the laboratory at Old Dominion University, frozen, and stored until analysis (see below). Sample analyses were conducted using the same methods described above for floodwater samples.

2.4. Sample analyses

We analyzed total dissolved nitrogen (TDN), ammonium (NH_4^+), nitrite (NO_2^-), nitrate (NO_3^-) + NO_2^- (NOx), and phosphate (PO_4^{3-}) concentrations using standard colorimetric methods. All concentrations were express in mg L^{-1} of N or P. NH_4^+ samples were analyzed within a week and the rest of the dissolved constituents were analyzed within a month of their collection. NH_4^+ concentrations were analyzed using the phenol hypochlorite method with spectrophotometric detection (Solorzano, 1969). PO_4^{3-}, NOx and NO_2^- were analyzed on an Astoria Pacific® nutrient autoanalyzer according to the manufacturer's specifications using standard colorimetric techniques (Grasshoff et al., 1999). Briefly, PO_4^{3-} was analyzed using the molybdenum blue method. NOx was measured by first reducing NO_3^- to NO_2^- using a cadmium coil and then NO_2^- was measured as an azo dye. $NO_2^-$was measured with the same technique, but without the cadmium coil. NO_3^- was calculated as the difference between NOx and NO_2^-. Dissolved inorganic nitrogen (DIN) was calculated as the sum of NOx and NH_4^+. Total dissolved nitrogen (TDN), samples were pretreated with potassium persulfate for complete oxidation of dissolved nitrogen compounds to NO_3^- (Valderrama, 1981). Oxidized samples were then analyzed to measure NO_3^-concentrations as described above. A glutamic acid ($C_5H_9NO_4$) standard was used to corroborate that the efficiency of the oxidation step was above 95%. Dissolved organic nitrogen (DON) was calculated as the difference between TDN and DIN. For all the dissolved nutrients measured, deionized water (DIW) was used as an instrument blank and to determine a reagent blank. Reagent blanks were treated the same as samples. Standards with concentrations at the low end of the standard curve were run every 10 samples to ensure the stability of sample runs. Detection limits ($3*\sigma$, $n>3$) were calculated for each instrumental run using repeat measurements of the lowest standard concentration. Samples with concentrations less than this were assigned the concentration of the calculated detection limit for the corresponding instrument run.

Enterococcus abundance was determined using Enterolert® kits (IDEXX Laboratories, Inc.), following the manufacturer's specifications by the Hampton Roads Sanitation District or the Virginia Department of Health. This method yields results in units of the most probable number (MPN) of cells, based on statistical probability, through a fluorescent indicator that is activated by *Enterococci* bacteria. The relationship between MPN and the number of colony forming units (CFU) is 1:1. Autoclaved pure water was used as a blank.

2.5. Data analysis

The Kolmogorov-Smirnov test was used to test for normality among different water quality variables in both floodwater and background estuarine waters. For all the datasets, residuals (each value minus the group mean) were not normally distributed. Therefore, the paired Wilcoxon signed-rank test was used to determine statistical differences between floodwater and background estuarine water concentrations for all of the water quality variables measured. The difference was

considered significant when $p < 0.05$. The median of the background samples was used as the paired value for the comparison. This value was considered to represent the background with a single value, due to the low spatial and temporal availability of riverine concentrations before the flooding campaign. When a significant difference was found between floodwater and estuarine concentrations, the one-tailed version of the paired Wilcoxon rank test was used to confirm which group of concentrations was higher.

2.6. Hydrodynamic model predictions of inundation volumes

The SCHISM hydrodynamic model was used to compute temporally and spatially resolved inundation maps (Zhang et al., 2016). A street-level hydrodynamic model was driven in a one-way nested configuration by SCHISM's predicted water levels prescribed as Dirichlet boundary conditions at Sewells Point near the Elizabeth River mouth to estimate water volumes and velocities throughout the cities of Norfolk, Portsmouth, and Chesapeake, including the Elizabeth and Lafayette Rivers (Loftis et al., 2018). This street-level model incorporates fluid fluxes, groundwater infiltration, and stormwater drainage infrastructure similar to other previously developed street-level models for nearby watersheds of coastal Virginia (Wang et al., 2015; Loftis et al., 2016). The geospatial inundation depth results from these models are presented as high-resolution time-aware GIS rasters of flood predictions prior to the 2017 king tide (Loftis et al., 2019). Hourly inundation depths from 36 h simulation results beginning at 06:00 on November 4, 2017, and ending at 18:00 on November 5, 2017, from SCHISM and the street-level model were used to estimate water volumes from GIS raster outputs at 1-meter resolution scale for this study (Danielson et al., 2016).

2.7. Nutrient loading calculations

We calculated the amount of N and P entering the Lafayette River during a single flooding event using an estimation of the volume of water inundating the landscape calculated from the aforementioned hydrodynamic models, and the difference in concentrations of dissolved nutrients in the floodwater samples and median concentrations measured from the adjacent estuarine water previous to the flooding event.

For the nutrient loading estimates, floodwater concentrations were pooled and the median concentration was calculated (to reduce the influence of outliers), while the background riverine concentration was calculated as the median of surface (<0.25 m) concentrations measured at a time series site near the mouth of the Lafayette River. The median of each group was used to avoid biasing by extreme low and high measurements. Nutrient inputs from floodwater to the estuary were calculated only when concentrations were statistically higher in the floodwaters doing a paired Wilcoxon signed-rank test (see above). To calculate the volume of floodwater, inundation depths were extracted from the predictive model's GIS raster outputs for the peak inundation period (13:36 UTC on November 4, and 13:36 UTC on November 5, 14:30 UTC) by computing the difference between values from the same lidar-derived digital elevation model of the Chesapeake Bay used by the hydrodynamic models (Danielson et al., 2016) and water surface elevation data for locations where water level sensors are located near the study site (Loftis et al., 2017).

3. Results and discussion

To our knowledge, this is the first estimate of nutrient loading to the Chesapeake Bay (or anywhere) as a result of tidal flooding. Such a loading calculation has not been made previously because it is difficult to gather enough samples in the right places at the right times and over appropriate timescales. A confluence of events and sampling programs enabled this project. We summarize them here to both advance our ability and improve our methods for quantifying nutrient loading resulting from tidal flooding. Tidal flooding is increasing in the mid-Atlantic region as a result of climate change and sea level rise (Ezer et al., 2013; Ezer and Atkinson 2014; Ezer 2018). The "King Tide" mapping event provided us with an unprecedented opportunity to calculate floodwater inundation volumes at a street level for the Lafayette River watershed (Loftis et al., 2019). In order to make an accurate assessment of nutrient concentrations in floodwaters, it was paramount that we collect many floodwater samples over a short period of time (at high tide and shortly thereafter) to characterize the natural variability in floodwater nutrient concentrations over diverse land uses at a watershed scale. Enlisting/recruiting a subset of the army of volunteers participating in the king tide mapping event enabled our synoptic water sampling. The Lafayette River is a small watershed, completely within the City of Norfolk and the one for which there is a TMDL. This made it possible for us to estimate nutrient loading at a watershed scale, on a relevant to the Chesapeake Bay restoration and the EPA's TMDL. The proximity of this Chesapeake Bay sub-watershed to Old Dominion University enabled us to transport samples to the laboratory in less than one hour where they could be processed for later analysis (see methods section). Finally, we needed high-quality estuarine observations against which to compare our floodwater measurements. This was made possible through our time-series sampling site in the Lafayette River associated with our harmful algal bloom monitoring program.

3.1. Dissolved nutrient concentrations in floodwater

Volunteers collected 190 floodwater samples from the Lafayette River watershed during the sampling campaign held during the perigean spring tide (i.e., king tide) on November 5, 2017 (Fig. 2). Overall, NOx-N and NH_4^+-N concentrations were higher in the floodwaters collected near the mouth of the estuary than from samples collected at the middle and upper part of the Lafayette River (Fig. 2A and C), while PO_4^{3-}-P and DON—N showed an opposite pattern, with higher concentrations in floodwater samples collected at the head of the system (Fig. 2B and D). Floodwater samples showed a large range in concentrations of dissolved constituents (Fig. 2A–D and Table 1). The average NH_4^+-N concentration in floodwater samples was 0.017 ± 0.032 mg L^{-1} (Table 1). More than 50% of the samples were lower than 0.013 mg L^{-1}, while 47% of the samples had concentrations between that and 0.056 mg L^{-1}, and the remaining 3% of the samples had concentrations above 0.056 mg L^{-1} (Table 1). The median, minimum, and maximum NOx-N concentrations were 0.094, 0.001, and 1.92 mg L^{-1}, respectively (Table 1). NO_3^--N represented > 80% of the NOx-N in 191 of the 194 samples collected and between 50 and 80% of the NOx-N in the remaining 3 samples. Concentrations of TDN—N in floodwater samples ranged from ~0.042 to 1.99 mg L^{-1}, with a mean and median of 0.473 (±0.349) and 0.43 mg L^{-1}, respectively (Table 1). Estimated values of DIN—N and DON—N ranged from ~0.002 to ~1.96 mg L^{-1}, with an average of 0.13 (±0.349) and 0.379 (±0.349), respectively (Table 1). PO_4^{3-}-P showed a broad range of concentrations (from 0.015 to 3.94 mg L^{-1}), but 98% of the samples had concentrations lower than 0.217 mg L^{-1}, with an average concentration of 0.082 (±0.29) mg L^{-1} (Table 1).

The differences between nutrient concentrations in floodwaters and the estuarine system, and the spatial variability observed in floodwater nutrient concentrations (Fig. 2) were likely influenced by several factors. These include factors known to affect nutrient runoff such as: (1) land use and the condition of the landscape at the time of flooding, and (2) the frequency, intensity, and amount of rainfall "washing" the landscape prior to or during the flood event; as well as factors more specific to tidal flooding such as: (1) the extent of flooding, (2) the associated length of time floodwaters remain on and interact with the landscape, (3) the frequency of flooding over previous tidal cycles, and (4) the variability in estuarine conditions prior to flooding events.

The quality and quantity of nutrient inputs from runoff can also vary

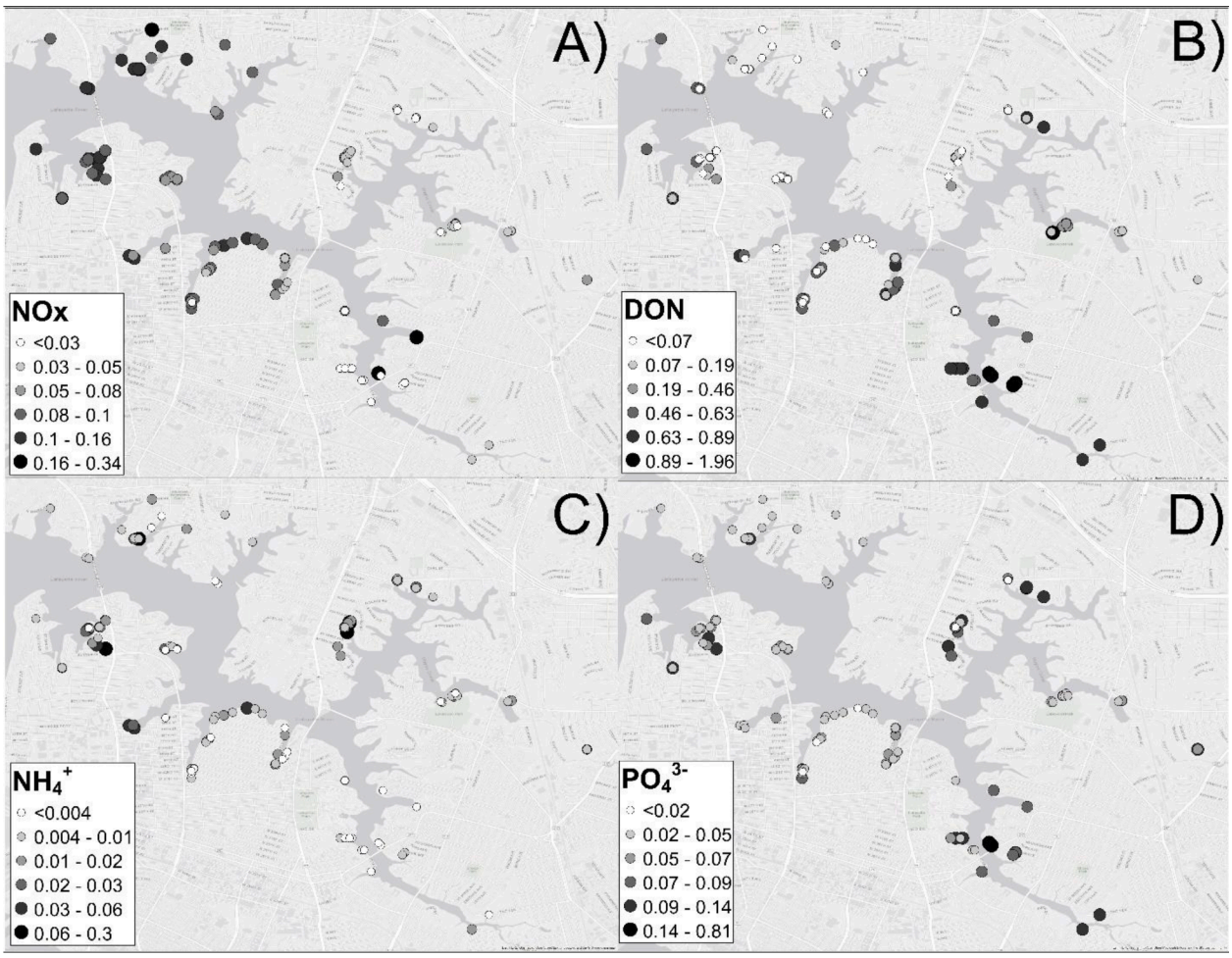

Fig. 2. The concentration of (A) NOx-N, (B) DON—N, and (C) NH_4^+-N, and (D) PO_4^{3-}-P, all in mg L^{-1}, in floodwater samples collected by citizen-science volunteers during the perigean spring tide of November 5, 2017.

Table 1
Comparison of dissolved nutrients concentrations (all in mg L^{-1}) in the Lafayette River estuary prior to flooding and in floodwater samples collected during the retreating king tide on November 5, 2017.

Variable		n	min	max	mean	SD (±)	median	*p*-value
TDN—N	**Floodwater**	164	0.052	1.989	0.475	0.349	0.430	
	In River*	35	0.525	1.071	0.750	0.123	0.741	2.3×10^{-17}
DON—N	**Floodwater**	152	0.0031	1.961	0.379	0.349	0.372	
	In River*	35	0.399	0.848	0.619	0.091	0.630	4.1×10^{-16}
DIN—N	**Floodwater***	181	0.0021	1.940	0.130	0.153	0.106	
	In River	39	0.0032	0.554	0.118	0.123	0.077	1.6×10^{-30}
NH_4^+-N	**Floodwater***	181	0.0004	0.305	0.017	0.032	0.0094	
	In River	39	0.0001	0.059	0.017	0.019	0.0089	0.0014
NOx-N	**Floodwater***	189	0.011	1.921	0.115	0.146	0.095	
	In River	39	0.00196	0.494	0.100	0.118	0.063	1.3×10^{-16}
PO_4^{3-}-P	**Floodwater**	190	0.015	3.937	0.082	0.289	0.047	
	In River*	39	0.013	0.127	0.068	0.030	0.077	4.4×10^{-17}

* Variables for which there was a significant difference ($p<0.05$) between floodwater and estuarine concentrations. The presence of the asterisk indicates which group had statistically higher concentrations for a given constituent and the p-value for each one-tailed Wilcoxon test is given.

with land use because activities undertaken on the adjacent landscape influences the type of materials on the landscape (e.g., hydrocarbons, fecal material, fertilizer, other chemical contaminants, etc.) and their transport to adjacent waterways (e.g., pervious versus impervious surface) (Wu et al., 2016). Of the landscape flooded in the Lafayette River watershed when tidal height is 1 m above mean lower low water (MLLW), 45.6% is residential (Fig. 3A), 13.6% is transportation (e.g., roads), 12.5% is recreation (e.g., parks), 8% is industrial (e.g., warehouses), 7.7% is institutional (e.g., schools), and 4.6% is commercial (e.g., restaurants) land use (Fig. 3A). Despite the increase in recreational and industrial land uses towards the head of the Lafayette River (Fig. 3A), we observed no consistent relationship between land use and floodwater nutrient concentrations for any of the dissolved constituents measured (Fig. 3B–D). This could be because the land use classifications used in this study were too broad or failed to distinguish important differences within categories. For example, residential land uses include green and gray areas, (e.g., grass and pavement), and a military facility was classified as residential. Institutional and recreational land uses

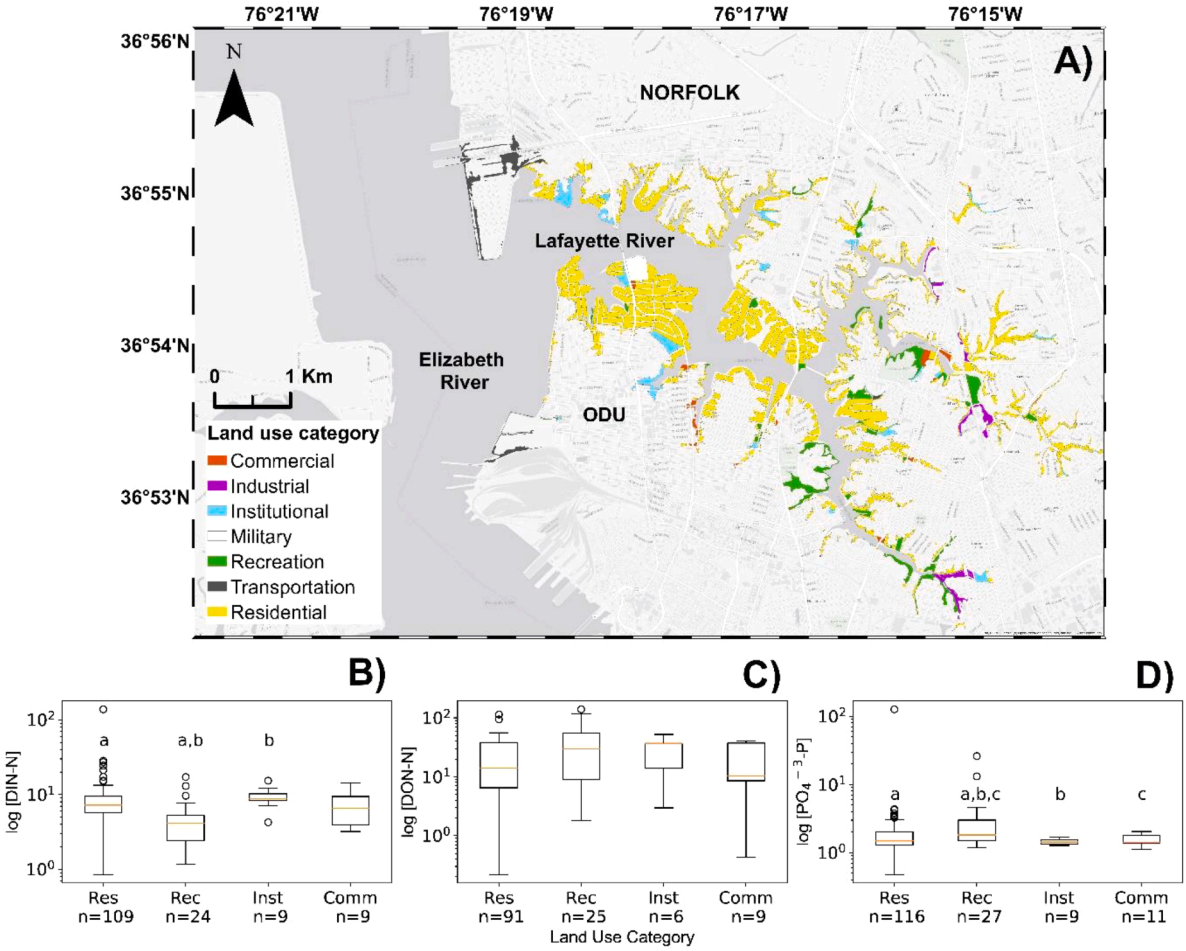

Fig. 3. (A) Land use designations, within the Lafayette River watershed, affected during the 2017 perigean spring tide, as in Fig. 1. Colors represent the land use category. Data source for land use category: City of Norfolk – Open Data Portal (https://www.norfolk.gov/3885/Open-Data-Norfolk). (B) DIN—N, (C) DON—N, and (D) PO_4^{3-}-P concentrations converted into a log scale in floodwater collected from areas designated as residential (Res), recreational (Rec), institutional (Inst) or commercial (Comm) land uses. The orange line within each box represents the median of the group. Whiskers represent the standard deviation of each group. Letters indicate land use categories between which there was a statistical difference ($p<0.05$, unpaired Wilcoxon test) for a given dissolved component. The number of samples collected within each land use category, for a given nutrient concentration, is shown (n) (For interpretation of the references to color in this figure legend, the reader is referred to the web version of this article.).

were also diverse; the institutional category included a museum garden and a country club, and the recreational designation included a zoo with direct connection to the Lafayette River. Future research should consider evaluations of how nutrient loading from tidal flooding varies by specific land uses. Such an analysis was beyond the scope of this study.

Estuarine systems are characterized by salinity gradients that reflect mixing between fresh and salt water end-members, which can shape nutrient distributions (Eyre and Balls, 1999). Because the Lafayette River is shallow and freshwater inputs are limited to runoff and groundwater, the salinity gradient in this system is primarily influenced by the tides and storms. Most of the time the salinity gradient is relatively small, and the difference between salinity near the headwaters and the mouth of the system is not more than 3 salinity units (Morse et al., 2011). Because the salinity gradient in the river is small, we relied on nutrient concentrations measured nearly daily at a timeseries site near the mouth of the river for our pre-flood in-estuary concentration estimates. While ideally, paired comparisons of floodwater and pre-flood, in-estuary nutrient concentrations adjacent to each flooded area would be optimal, they were beyond the scope of this study. Further research is needed to better characterize variability in estuarine nutrient concentrations prior to flooding events.

In addition to direct loading of nutrients, differences in dissolved nutrient concentrations between estuarine and floodwater samples can occur as a result of nutrient transformation as floodwaters interact with the landscape. According to Ezer (2018), the number of hours that water levels were 0.53 m above mean higher high water (MHHW) in Norfolk, VA, in 2016 was ~90 h. The same author report that this number has increased dramatically over the last 50 years and is projected to increase at an accelerating rate in the future. Although there are no studies to our knowledge reporting on floodwater-soil biogeochemical interactions in urbanized areas, changes in water chemistry have been observed in association with more rural systems (e.g., Weissman and Tully, 2020). In this study, DON—N concentrations were higher in the estuary than in floodwaters, while DIN—N showed an opposite trend (Fig. 4). This could mean that higher DIN—N concentrations in floodwaters were due to remineralization of DON to NH_4^+, NO_2^- and NO_3^-, during the period when the landscape was inundated, rather than being due to their direct addition from materials being transported from the land. For example, Ardón et al. (2013) found that repeated saltwater intrusion during tidal flooding events changed N export from being dominated by organic N to being dominated by inorganic N in wetland sediments. Although reported rates of DIN regeneration from DON, and other nitrogen cycle processes, show that microbial transformations are fast enough to make measurable changes over the time span in which floodwaters remains on land (Herbert, 1999), we do not know the extent to which they do so during tidal flooding events inundating urban landscapes. Future studies

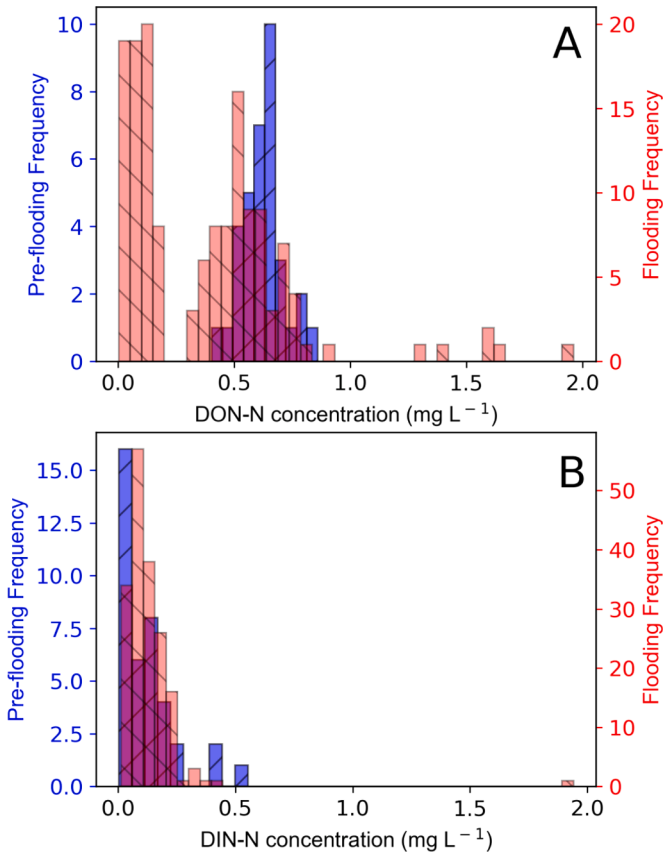

Fig. 4. Absolute frequency of DON- and DIN—N concentrations in floodwater (red) and in-river (blue) samples. See Table 1 for a detailed description of the distributional parameters of this dissolved nutrient and the results of the statistical analysis comparing floodwater and background concentrations. (For interpretation of the references to color in this figure legend, the reader is referred to the web version of this article.)

should examine nutrient transformations (e.g., ammonification and nitrification rates) in inundated soils and floodwater to better understand the sources and fates of nutrients during tidal flooding events.

3.2. Dissolved nutrient inputs during tidal flooding

For all of the analytes measured here, the maximum concentrations in floodwaters were more than 2 to 10 times higher than those measured in the estuary at our timeseries site (Table 1). However, only concentrations of DIN—N in floodwaters were statistically higher than pre-flood estuarine samples ($p<0.05$, paired Wilcoxon, Table 1). Average DON—N, TDN—N, and PO_4^{3-}-P concentrations were statistically higher in estuarine waters than in the floodwater samples (Table 1).

From the LIDAR-derived digital elevation model and corrections from water surface elevation measurements in the Lafayette River, we estimated that about $3.9 \times 10^{10} \pm 1.6 \times 10^{9}$ L of estuarine water inundated the landscape along the perimeter of the Lafayette River during the perigean spring tide on November 5, 2017, making the inundation prediction model's uncertainty during this tidal inundation simulation approximately 4.2%. Only DIN—N concentrations were used to estimate nutrient inputs because this variable was the one in which concentrations were statistically higher in floodwaters than in the estuary itself and because the TDN—N results, and thus the DON—N concentrations, were highly variable (Table 1). The difference between the median DIN—N concentrations in floodwater and the estuary was 0.0294 mg N L^{-1}. Multiplying this concentration by the volume of floodwater inundating the perimeter of the Lafayette River during the sampling event, we estimate that about 1145 kg of N was introduced to the system in the form of DIN during this single, blue-sky flooding event.

According to the Environmental Protection Agency (EPA), the land-based annual load allocation for N to the Lafayette River should be less than 880 kg $year^{-1}$ ((Table 9–1; EPA, 2010). Thus, based on our calculations, this single flooding event delivered about 30% more of the annual load allocation for this category to the Lafayette River. While our results are provocative, they must be considered carefully for several reasons. First, all flooding events are not equal; tidal height and the extent of inundation varies between flooding events, and the condition of the inundated landscape can also vary depending on a variety of factors (e.g., seasonality, length of time since last rainfall/flooding, and land use). The water level the day of the flooding event during which we collected samples, although high enough to inundate the streets close to the estuary (Fig. 1), was not the as high as predicted or as high as other flooding events in the region during 2017 (Fig. 5). During the past century, the tide gage located close to the mouth of the Lafayette River has registered flooding events as high as 1.9 m above MLLW (Fig. 5). Further, the estuarine condition is also highly variable and nutrient concentrations can vary on short temporal and spatial scales (Morse et al., 2014).

The floodwater nutrient anomalies presented here were calculated assuming homogenous nutrient concentrations within the estuary prior to the tidal flooding and using measurements collected several days before the sampling event at a site near the mouth of the tributary (Fig. 1). However, concentrations of dissolved constituents in the Lafayette River water can vary on multiple spatial and temporal scales, depending on weather (e.g., rainfall and wind; Morse et al., 2014; Egerton et al., 2014; Filippino et al., 2017), biogeochemical seasonality (Mulholland et al., 2009, 2018), and changes in estuarine water transport (Morse et al., 2011, 2013). Thus, our approach could over- or under-estimate floodwater nutrient fluxes if background concentrations decreased or increased relative to the median value used for our calculations. This variability could confound our ability to determine nutrient loads accurately during individual flooding events. While we had many synoptic floodwater samples, we had few in-estuary nutrient concentration measurements just prior to the tidal flooding. We recommend incorporating pre-flood sampling along the length of the estuary to provide better-paired comparisons of floodwater versus estuarine nutrient concentrations. Sampling estuarine conditions immediately before each flooding event would also allow us to account for the variability associated with biogeochemical and ecological seasonality that has been observed in this estuarine system (Morse et al., 2014; Egerton et al., 2014; Mulholland et al. 2018).

Overall, this study points to "blue sky" flooding as a potentially significant source of nutrients to estuarine and coastal systems. This is not surprising as nutrient inputs from overland stormwater runoff are known to be significant (Hale et al., 2015). As sea levels continue to rise in many coastal areas around the globe (Haigh et al., 2014), water level-induced transport of materials from the landscape to the connected waterways will likely increase in coastal watersheds unless measures are taken to prevent these transports. Increases in the intensity, frequency, and duration of harmful algal blooms (HABs), and expansion of hypoxic waters in the Chesapeake Bay have been attributed to more than 100 years of intense nutrient loading to the system (Kemp et al., 2005). Sea level rise and associated increases in tidal flooding may exacerbate nutrient loading. The Chesapeake Bay restoration and similar efforts in other coastal waterways along the eastern seaboard of the U.S. have implemented both voluntary and mandatory nutrient reduction actions to achieve water quality goals. These efforts will be jeopardized if nutrient loads delivered as a result of coastal flooding are ignored and strategies for reducing these loads are not adopted, particularly in hot spots for water quality impairments such as the Lafayette River. The Lafayette River has been identified as an initiation site for harmful algal blooms (HABs) and these have been linked to N inputs (Morse et al., 2011, 2013, 2014; Mulholland et al., 2018). Similarly, links between nutrient inputs and HABs have been observed throughout the

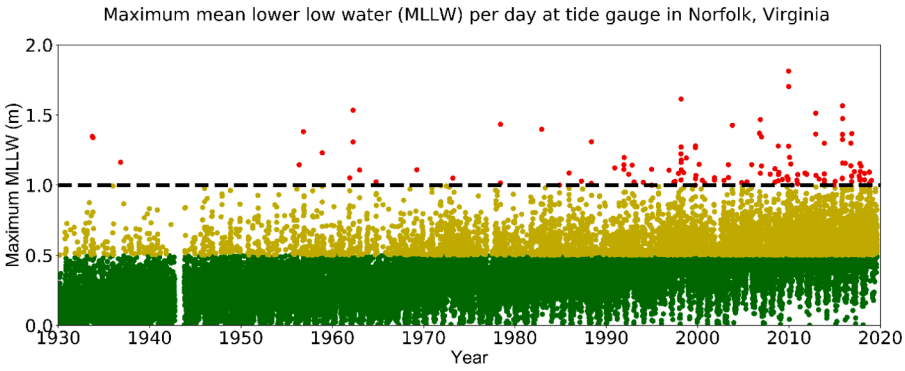

Fig. 5. Maximum water levels measured between 1930 and 2019 at the Sewells Point station, Norfolk, VA. Green dots (MLLW <0.5 m) are considered a 'no flooding scenario', while yellow (MLLW 0.5 - 1 m) and red dots (MLLW >1 m) are water levels that produce flooding in this region as exemplified in Fig. 1. The dotted line shows the water level during our sampling campaign. Data source: NOAA's Tides & Currents (https://tidesandcurrents.noaa.gov) (For interpretation of the references to color in this figure legend, the reader is referred to the web version of this article.).

Chesapeake Bay watershed and other coastal areas around the globe (see Wells et al., 2015 and references therein).

3.3. Microbial contamination in floodwaters

The median and average abundance of *Enterococcus* was 1220 and 6283 ± 8984 MPN 100 mL^{-1}, respectively, with results ranging from 30 to >24,000 MPN 100 mL^{-1} (Fig. 5). Further, the maximum detectable concentration of 24,000 MPN 100 mL^{-1}, the upper limit of analytical detection for the method, was observed in ~17% of the samples collected. There was no clear spatial pattern in *Enterococcus* abundance (Fig. 6).

Enterococcus spp. is a general fecal indicator shed by a variety of organisms into the environment during excretion (Franzetti et al., 2004). Its abundance in the environment has been associated with human health risks since the last century, which has made it the default indicator for fecal contamination (Cabelli et al., 1982). Transmission to humans can occur either by consuming or having contact with contaminated objects or water (Enayati et al., 2015; Iversen et al., 2004). In this study, *Enterococcus* in floodwaters were far in excess of standards established for recreational waters by the US Environmental Protection Agency (Fig. 7). This standard recommends concentrations be no higher than 104 colony forming units (CFU) per 100 mL of water to achieve an estimated illness rate of 36 per 1000 people (Recreational Water Quality Criteria by EPA, 2012). Only 5% of the samples collected during our study met this standard, while the remaining samples had concentrations that were one to two orders of magnitude higher than this standard (Fig. 7). Consistent with our results, Gidley et al. (2016) found high fecal contamination indicators (e.g., human bacteroidales) in floodwaters and at drains where floodwaters were rising to inundate the streets in Miami Beach, FL, USA. ten Veldhuis et al., 2010 found that riverine flooding induced by excessive precipitation resulted in increases in the abundances of fecal indicators in floodwaters on the order of those found in untreated wastewater, ranging from 5×10^4 to 1×10^7 CFU 100 mL^{-1}.

Sources of *Enterococcus* bacteria include warm-blooded animals such as ducks, geese, dogs, and gulls, however high abundances of *Enterococci* have been found in areas without obvious sources (Byappanahalli et al., 2012). In the Lafayette River watershed, several dog parks in the residential areas along the perimeter of the Lafayette River are affected by tidal flooding. In addition, ducks, geese, and gulls are commonly observed in floodwaters and could be sources of *Enterococcus* contamination. Another source of *Enterococcus* could be the transport or reproduction of bacteria during the intrusion of floodwater through storm drains. Haile et al. (1999) found that biofilms developing within the drainage systems can increase fecal contamination indicators in floodwater during tidal flooding events. In urban areas affected by tidal flooding, such as Norfolk, Virginia, much of the water that inundates the landscape passes through the storm drain system (e.g., Shen et al., 2019).

While it is difficult to quantify, people are frequently in contact with floodwater during flooding events. In urban areas, the most common exposures include contact with floodwaters while walking through affected areas to get to cars, homes, businesses, schools, and other

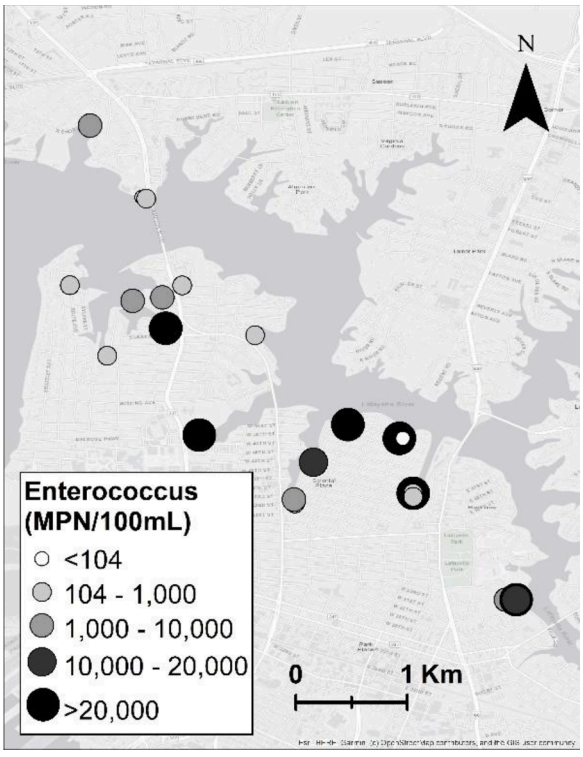

Fig. 6. *Enterococcus* abundance (in MPN 100 mL^{-1}) in floodwater samples collected by citizen-science volunteers during the perigean spring tide of November 5, 2017.

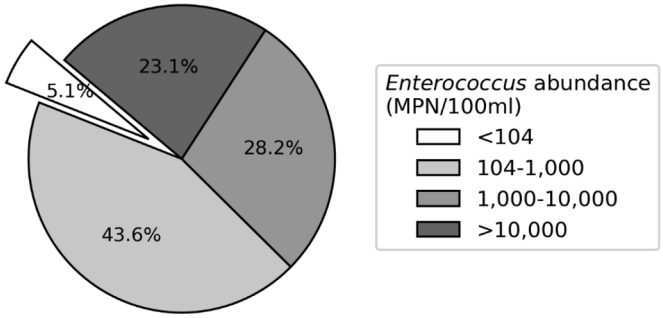

Fig. 7. Percentage of floodwater samples with ≤ 104 (EPA standard), 105–1000, 1000–10,000, or > 10,000 MPN 100 mL^{-1} of *Enterococcus*.

destinations, and contact with items (e.g., outerwear) that have been in contact with floodwater. The dominant land use along the perimeter of the Lafayette River is residential (Fig. 3A), which could increase the number of people in contact with floodwater and the contaminants it carries. The large and increasing fraction of human populations living in coastal areas coupled with increases in tidal flooding due to sea level rise suggests that more people will be increasingly affected by flooding and exposed to potential contaminants carried by floodwaters (Neumann et al., 2015). Future research should consider not only the nutrient loads delivered to coastal waters but also the effects of tidal flooding on human health through exposure to waterborne pathogens.

4. Conclusions

Despite the impact that tidal flooding has in coastal areas, the effects of these events on water quality have not been examined. In this study, we carried out the first comprehensive spatial characterization of nutrient and fecal material concentrations in floodwaters from an urbanized Chesapeake Bay sub-estuary. The main conclusions of this study are as follows:

- DIN—N concentrations were statistically higher in floodwaters than in adjacent estuarine waters, indicating that coastal flooding is a previously unquantified, and substantial source of nutrients to coastal and estuarine systems.
- Enhanced biogeochemical processes in the floodwater itself or the direct transport of dissolved nitrogen from the landscape to estuarine waters could explain the differences between floodwater and estuarine concentrations.
- *Enterococcus* abundance exceeded the recommended standard for recreational waters in nearly all of the floodwaters examined suggesting that contact with floodwaters can be harmful to public health.

Results from this study suggest that DIN transport into adjacent water bodies by floodwaters may be high. Thus, failing to consider nutrient fluxes resulting from tidally induced inundations could result in underestimates of nutrient inputs into coastal waters. Their exclusion could bias water quality model projections of nutrient loads to coastal areas thereby jeopardizing mitigation, conservation, and restoration efforts. Further research should be done to confirm these estimates and their variability with respect to land use, meteorology, and variability in landscape conditions.

Declaration of Competing Interest

The authors declare that they have no known competing financial or personal interests influencing this research.

Acknowledgments

We would like to thank the Hampton Roads Sanitation District (HRSD) for funding. In addition, many graduate students, faculty, staff, and undergraduate students from the Ocean and Earth Sciences department and other departments at Old Dominion University. We would like to thank students, parents, and staff from Maury High School for their assistance during sampling. Thanks to Kyle Spencer, from the City Manager's Office of Resilience, Norfolk, VA, for the water level data he supplied for the inundation model. Thanks also to HRSD and Virginia Department of Health (VDH) for their analyses of *Enterococcus*.

References

Akpinar-Elci, M., Rose, S., Kekeh, M., 2018. Well-being and mental health impact of household flooding in Guyana, the Caribbean. Mar. Technol. Soc. J. 52 (2), 18–22. https://doi.org/10.4031/MTSJ.52.2.3.

Ardón, M., Morse, J.L., Colman, B.P., Bernhardt, E.S., 2013. Drought-induced saltwater incursion leads to increased wetland nitrogen export. Glob. Chang. Biol 19, 2976–2985. https://doi.org/10.1111/gcb.12287.

Boon, J., Mitchell, M., 2015. Nonlinear change in sea level observed at North American tide stations. J. Coast. Res. 31 (6), 1295–1305. http://www.jstor.org/stable/43598459.

Boon, J.D., Mitchell, M., Loftis, J.D., Malmquist, D.M., 2018. Anthropocene sea level change: a history of recent trends observed in the U.S. east, gulf, and west coast regions. Spec. Rep. Appl. Mar. Sci. Ocean Eng. (SRAMSOE) 467. https://doi.org/10.21220/V5T17T.

Bristow, L.A., Mohr, W., Ahmerkamp, S., Kuypers, M.M.M., 2017. Nutrients that limit growth in the ocean. Curr. Biol. 27 (11), R474–R478. https://doi.org/10.1016/j.cub.2017.03.030.

Byappanahalli, M.N., Nevers, M.B., Korajkic, A., Staley, Z.R., Harwood, V.J., 2012. *Enterococci* in the Environment. Microbiol. Mol. Biol. Rev. 76 (4), 685–706. https://doi.org/10.1128/MMBR.00023-12.

Cabelli, V.J., Dufour, A.P., McCabe, L.J., Levin, M.A., 1982. Swimming-associated gastroenteritis and water quality. Am. J. Epidemiol. 115 (4), 606–616. https://doi.org/10.1093/oxfordjournals.aje.a113342.

Ching-Pong, M.P., Zaili, Y., Delia, D., Zhuohua, Q., 2018. Review on seaport and airport adaptation to climate change: a case on sea level rise and flooding. Mar. Technol. Soc. J. 52 (2), 23–33. https://doi.org/10.4031/MTSJ.52.2.4 (11).

Danielson, J.J., Poppenga, S.K., Brock, J.C., Evans, G.A., Tyler, D.J., Gesch, D.B., Thatcher, C.A., Barras, J.A., 2016. Topobathymetric elevation model development using a new methodology: coastal national elevation database. J. Coast. Res. 76, 75–89. https://doi.org/10.2112/SI76-008.

Downing, J.A., 1997. Marine nitrogen: phosphorus stoichiometry and the global N:P cycle. Biogeochemistry 37, 237–252. https://doi.org/10.1023/A:1005712322036.

Egerton, T.A., Morse, R.E., Marshall, H.G., Mulholland, M.R., 2014. Emergence of algal blooms: the effects of short-term variability in water quality on phytoplankton abundance, diversity, and community composition in a tidal estuary. Microorganisms 2, 33–57. https://doi.org/10.3390/microorganisms2010033.

Enayati, M., Sadeghi, J., Nahaei, M., Aghazadeh, M., Pourshafie, M., Talebi, M., 2015. Virulence and antimicrobial resistance of Enterococcus faecium isolated from water samples. Lett. Appl. Microbiol. 61, 339–345. https://doi.org/10.1111/lam.12474.

Environmental Protection Agency (EPA), 2010. Chesapeake Bay TMDL document. last visited in December of 2018. https://www.epa.gov/chesapeake-bay-tmdl/chesapeake-bay-tmdl-document.

Eyre, B.D., Balls, P., 1999. A comparative study of nutrient behavior along the gradient of tropical and temperate estuaries. Estuaries 22 (2A), 313–326. https://doi.org/10.2307/1352987.

Ezer, T., Corlett, W.B., 2012. Is sea level rise accelerating in the Chesapeake Bay? A demonstration of a novel new approach for analyzing sea level data. Geophys. Res. Lett. 39, L19605. https://doi.org/10.1029/2012GL053435.

Ezer, T., Atkinson, L.P., Corlett, W.B., Blanco, J.L., 2013. Gulf Stream's induced sea level rise and variability along the US mid-Atlantic coast. J. Geophys. Res. Oceans 118, 685–697. https://doi.org/10.1002/jgrc.20091.

Ezer, T., Atkinson, L.P., 2014. Accelerated flooding along the U.S. East coast: on the impact of sea-level rise, tides, storms, the Gulf Stream, and the North Atlantic Oscillations. Earth's Future 2 (8), 362–382. https://doi.org/10.1002/2014EF000252.

Ezer, T., 2018. The increased risk of flooding in hampton roads: on the roles of sea level rise, storm surges, hurricanes, and the gulf stream. Mar. Technol. Soc. J. 52 (2), 34–44. https://doi.org/10.4031/MTSJ.52.2.6.

Filippino, K.C., Egerton, T.A., Hunley, W.S., Mulholland, M.R., 2017. The influence of storms on water quality and phytoplankton dynamics in the Tidal James river. Estuaries Coasts 40, 80–94. https://doi.org/10.1007/s12237-016-0145-6.

Franzetti, L., Pompei, M., Scarpellini, M., Galli, A., 2004. Phenotypic and genotypic characterization of Enterococcus spp. of different origins. Curr. Microbiol. 49 (4), 255–260. https://doi.org/10.1007/s00284-004-4242-6.

Gidley, M., Briceño, H.O., Serna, A., Kelly, E., Sinigalliano, C., 2016. Characterizing Microbial Water Quality of extreme tide floodwaters discharged from an urbanized subtropical beach: case study of miami beach with implications for sea level rise and public health. ASLO 2016 Ocean Sciences Meeting, New Orleans, Louisiana, February 23, 2016 2016. Abstract ID: MM24C-0460.

Grasshoff, K., Kremling, K., Ehrhardt, M. (Eds.), 1999. Methods of Seawater Analysis, 3rd Ed. Verlag Chemie, Weinheim/Deerfield Beach, Florida, pp. 159–208. https://doi.org/10.1002/iroh.19850700232. 1983.

Hagy, J.D., Boyton, W., Keefe, C., Wood, K., 2004. Hypoxia relation in chesapeake Bay, 1950-2001 long-term to nutrient loading and river flow. Estuaries 27 (4), 634–658. JSTOR. www.jstor.org/stable/1353476.

Haigh, I.D., Wahl, T., Rohling, E.J., Price, R.M., Pattiaratchi, C.B., Calafat, F.M., Dangendorf, S., 2014. Timescales for detecting a significant acceleration in sea level rise. Nat. Commun. 5, 3635. https://doi.org/10.1038/ncomms4635.

Haile, R., Witte, J., Gold, M., Cressey, R., McGee, C., Millikan, R., Glasser, A., Harawa, N., Ervin, C., Harmon, P., Harper, J., Dermand, J., Alamillo, J., Barrett, K., Nides, M., Wang, G., 1999. The health effects of swimming in ocean water contaminated by storm drain runoff. Epidemiology 10 (4), 355–363. http://www.jstor.org/stable/3703553.

Hale, R.L., Grimm, N.B., Vörösmarty, C.J., Fekete, B., 2015. Nitrogen and phosphorus fluxes from watersheds of the northeast U.S. from 1930 to 2000: role of anthropogenic nutrient inputs, infrastructure, and runoff. Glob. Biogeochem. Cycles 29 (3), 341–356. https://doi.org/10.1002/2014GB004909.

Herbert, R.A., 1999. Nitrogen cycling in coastal marine ecosystems. FEMS Microbiol. Rev. 23 (5), 563–590. https://doi.org/10.1111/j.1574-6976.1999.tb00414.x.

Iversen, A., Kühn, I., Rahman, M., Franklin, A., Burman, L.G., Olsson-Liljequist, B., Torell, E., Möllby, R., 2004. Evidence for transmission between humans and the environment of a nosocomial strain of Enterococcus faecium. Environ. Microbiol. 6 (1), 55–59. https://doi.org/10.1046/j.1462-2920.2003.00534.x.

Kemp, W.M., Boynton, W., Adolf, J., Boesch, D., Boicourt, W., Brush, G., Cornwell, J., Fisher, T., Glibert, P., Hagy, J., Harding, L.W., Houde, E., Kimmel, D., Miller, W.D., Newell, R., Roman, M., Smith, E.M., Stevenson, J., 2005. Eutrophication of Chesapeake Bay: historical trends and ecological interactions. Mar. Ecol. Prog. Ser. 303, 1–29. https://doi.org/10.3354/meps303001.

Kleinosky, L.R., Yarnal, B., Fisher, A., 2007. Vulnerability of hampton roads, Virginia to storm-surge flooding and sea-level rise. Nat. Hazards 40, 43–70. https://doi.org/10.1007/s11069-006-0004-z.

Köhler, S., Jungkunst, H., Erasmi, S., Gerold, G., 2013. The effects of land use change on atmospheric nutrient deposition in central Sulawesi. Erdkunde 67 (2), 109–122. www.jstor.org/stable/23595392.

Li, H., Lin, L., Burks-Copes, K.A., 2013. Modeling of coastal inundation, storm surge, and relative sea-level rise at naval station norfolk, Norfolk, Virginia, U.S.A. J. Coast. Res. 29 (1), 18–30. https://doi.org/10.2112/JCOASTRES-d-12-00056.1.

Loftis, J.D., Wang, H.V., DeYoung, R.J., Ball, W.B., Brock, J.C., Gesch, D.B., Parrish, C.E., Rogers, J.N., Wright, C.W., 2016. Using lidar elevation data to develop a topobathymetric digital elevation model for sub-grid inundation modeling at langley research center, In:. Advances in Topobathymetric Mapping, Models, and Applications J. Coast. Res. Spec. Issue 76, 134–148. https://doi.org/10.2112/SI76-012.

Loftis, J.D., Wang, H., Forrest, D., Rhee, S., Nguyen, C., 2017. Emerging flood model validation frameworks for street-level inundation modeling with StormSense. In: Proceedings of the 2nd International Workshop on Science of Smart City Operations and Platforms Engineering SCOPE, pp. 13–18. https://doi.org/10.1145/3063386.3063764, 2(1).

Loftis, J.D., Forrest, D., Wang, H., Rogers, L., Molthan, A., Bekaert, D., Cohen, S., Sun, D., 2018. Communities and areas at intensive risk in the mid-atlantic region: a reanalysis of 2011 hurricane irene with future sea level rise and land subsidence. In: , pp. 1–7. https://doi.org/10.1109/OCEANS.2018.8604864.

Loftis, J.D., Mitchell, M., Schatt, D., Forrest, D.R., Wang, H.V., Mayfield, D., Stiles, W.A., 2019. Validating an operational flood forecast model using citizen science in hampton roads, VA, USA. J. Mar. Sci. Eng. 7 (8), 242. https://doi.org/10.3390/jmse7080242.

Morse, R.E., Shen, J., Blanco-Garcia, J.L., Hunley, W.S., Fentress, S., Wiggins, M., Mulholland, M.R., 2011. Environmental and physical controls on the formation and transport of blooms of the dinoflagellate cochlodinium polykrikoides margalef in the lower Chesapeake Bay and its tributaries. Estuaries Coasts 34 (5), 1006–1025. https://doi.org/10.1007/s12237-011-9398-2.

Morse, R.E., Mulholland, M.R., Hunley, W.S., Fentress, S., Wiggins, M., Blanco-Garcia, J. L., 2013. Controls on the initiation and development of blooms of the dinoflagellate *Cochlodinium polykrikoides* Margalef in lower Chesapeake Bay and its tributaries. Harmful Algae 28, 71–82. https://doi.org/10.1016/j.hal.2013.05.013.

Morse, R.E., Mulholland, M.R., Egerton, T.A., Marshall, H.G., 2014. Phytoplankton and nutrient dynamics in a tidally dominated eutrophic estuary: daily variability and controls on bloom formation. Mar. Ecol. Prog. Ser. 503, 59–74. https://doi.org/10.3354/meps10743.

Mulholland, M.R., Morse, R.E., Boneillo, G.E., Bernhardt, P.W., Filippino, K.C., Procise, L.A., Blanco-Garcia, J.L., Marshall, H.G., Egerton, T.A., Hunley, W.S., Moore, K.A., Berry, D.L., Gobler, C.J., 2009. Understanding causes and impacts of the dinoflagellate, cochlodinium polykrikoides, blooms in the Chesapeake Bay. Estuaries Coasts 32 (4), 734–747. https://doi.org/10.1007/s12237-009-9169-5.

Mulholland, M.R., Morse, R., Egerton, T., Bernhardt, P.W., Filippino, K.C., 2018. Blooms of dinoflagellate mixotrophs in a Lower Chesapeake Bay tributary: carbon and nitrogen uptake over diurnal, seasonal, and interannual timescales. Estuaries Coasts 41, 1744–1765. https://doi.org/10.1007/s12237-018-0388-5.

Neumann, B., Vafeidis, A.T., Zimmermann, J., Nicholls, R.J., 2015. Future coastal population growth and exposure to sea-level rise and coastal flooding-a global assessment. PLoS ONE 10 (3), e0118571. https://doi.org/10.1371/journal.pone.0118571.

Nicholls, R., Cazenave, A., 2010. Sea-level rise and its impact on coastal zones. Science 328 (5985), 1517–1520. https://doi.org/10.1126/science.1185782.

Pandey, J., Pandey, U., Singh, A.V., 2014. Impact of changing atmospheric deposition chemistry on carbon and nutrient loading to Ganga River: integrating land–atmosphere–water components to uncover cross-domain carbon linkages. Biogeochemistry 119, 179–198. https://doi.org/10.1007/s10533-014-9957-2.

Raposa, K.B., Wasson, K., Smith, E., Crooks, J.A., Delgado, P., Fernald, S.H., Ferner, M.C., Helms, A., Hice, L.A., Mora, J.W., Puckett, B., Sanger, D., Shull, S., Spurrier, L., Stevens, R., Lerberg, S., 2016. Assessing tidal marsh resilience to sea-level rise at broad geographic scales with multi-metric indices. Biol. Conserv. 204, 263–275. https://doi.org/10.1016/j.biocon.2016.10.015.

Selbig, W., 2016. Evaluation of leaf removal as a means to reduce nutrient concentrations and loads in urban stormwater. Sci. Total Environ. 571, 124–133. https://doi.org/10.1016/j.scitotenv.2016.07.003.

Shen, Y., Morsy, M.M., Huxley, C., Tahvildari, N., Goodall, J.L., 2019. Flood risk assessment and increased resilience for coastal urban watersheds under the combined impact of storm tide and heavy rainfall. J. Hydrol. 579, 124159 https://doi.org/10.1016/j.jhydrol.2019.124159 (Amst).

Solorzano, L., 1969. Determination of ammonia in natural waters by phenolhypochlorite method. Limnol. Oceanogr. 14 (5), 799–801, 10.4319/lo.1969.14.5.0799.

Spanger-Siegfried, E., Fitzpatrick, M.F., Dahl, K., 2014. Encroaching tides: How sea Level Rise and Tidal Flooding Threaten U.S. East and Gulf Coast Communities Over the Next 30 years. Cambridge, MA: Union of Concerned Scientists. University of Minnesota Digital Conservancy. Retrieved from the. http://hdl.handle.net/11299/189228.

Tebaldi, C., Strauss, B.H., Zervas, C.E., 2012. Modelling sea level rise impacts on storm surges along U.S. coasts. Environ. Res. Lett. 7 (1), 014032 https://doi.org/10.1088/1748-9326/7/1/014032.

ten Veldhuis, J.A.E., Clemens, F.H.L.R., Sterk, G., Berends, B.R., 2010. Microbial risks associated with exposure to pathogens in contaminated urban floodwater. Water Res. 44 (9), 2910–2918. https://doi.org/10.1016/j.watres.2010.02.009.

Valderrama, J.C., 1981. The simultaneous analysis of total nitrogen and total phosphorus in natural waters. Mar. Chem. 10, 109–122. https://doi.org/10.1016/0304-4203(81)90027-X.

Wainger, L.A., 2012. Opportunities for reducing total maximum daily load (TMDL) compliance costs: lessons from the Chesapeake Bay. Environ. Sci. Technol. 46, 9256–9265. https://doi.org/10.1021/es300540k.

Wainger, L.A., Van Houtven, G., Loomis, R., Messer, J., Beach, R., Deerhake, M., 2013. Tradeoffs among ecosystem services, performance certainty, and cost-efficiency in implementation of the Chesapeake Bay total maximum daily load. Agric. Res. Econ. Rev. 42 (1), 196–224. https://doi.org/10.1017/S1068280500007693.

Wang, H., Loftis, J.D., Forrest, D., Smith, W., Stamey, B., 2015. Modeling storm surge and inundation in Washington, D.C., during Hurricane Isabel and the 1936 Potomac River Great Flood. J. Mar. Sci. Eng. 3 (3), 607–629. https://doi.org/10.3390/jmse3030607.

Weissman, D.S., Tully, K.L., 2020. Saltwater intrusion affects nutrient concentrations in soil porewater and surface waters of coastal habitats. Ecosphere 11 (2). https://doi.org/10.1002/ecs2.3041.

Wells, M.L., Trainerm, V.L., Smayda, T.J., Karlson, B.S.O., Trick, C.G., Kudela, R.M., Ishikawa, A., Bernard, S., Wulff, A., Anderson, D.M., Cochlan, W.P., 2015. Harmful algal blooms and climate change: learning from the past and present to forecast the future. Harmful Algae 49, 68–93. https://doi.org/10.1016/j.hal.2015.07.009.

Wu, J., Franzen, D., Malmstrom, M.E., 2016. Nutrient flows following changes in source strengths, land use and climate in an urban catchment, Råcksta Träsk in Stockholm, Sweden. Ecol. Model. 338, 69–77. https://doi.org/10.1016/j.ecolmodel.2016.08.001.

Zhang, Y., Ye, F., Stanev, E.V., Grashorn, S., 2016. Seamless cross-scale modeling with SCHISM. Ocean Model. 102, 64–81. https://doi.org/10.1016/j.ocemod.2016.05.002.